

# A Comparison of the State of Stress at an Incomplete Fretting Contact Edge with a Crack Tip

J P J Truelove and D A Hills

*Department of Engineering Science, University of Oxford, Parks Road, OXFORD OX1 3PJ  
UK*

## Abstract

The similarity in implied process zones, based on violations of the plastic yield condition, between the state of stress at the edge of an incomplete contact subject to reciprocating shear and tension and a crack suffering pure mode II loading are compared. This is done for both small and large amounts of edge slip, i.e. when the frictional slip region is either enveloped by the plastic region or envelops it. The results show that for realistic coefficients of friction strong agreement is unlikely to occur, so that attempting to analyse the nucleation of fretting cracks as a form of crack branching/turning is inappropriate and the effect of normal load on crack nucleation is an important consideration.

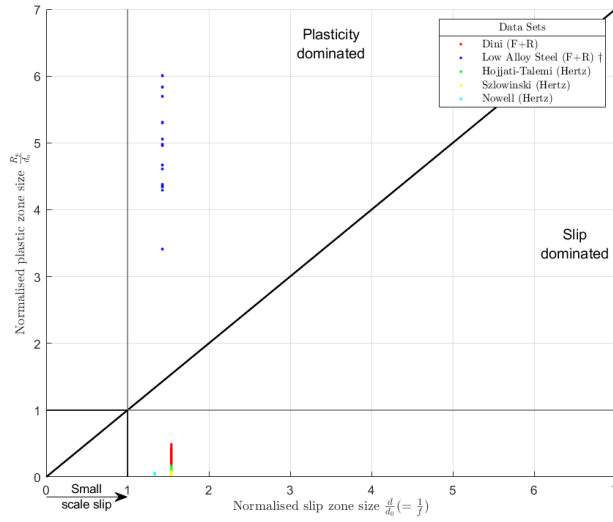


Figure 1: In this paper we demonstrate that in order for the contact edge to behave like a crack tip we require both the slip zone size,  $d$ , and the plastic radius,  $r_p$ , to be smaller than the internal length scale of the asymptote,  $d_0$ . In the figure above results for a range of tests are plotted, showing that while the plastic radius falls within the region  $r_p < d_0$  for the majority of tests, there are no tests where the slip zone falls within the region  $d < d_0$ .

*Keywords:* Contact Mechanics, Fretting, Plastic

---

## **Nomenclature**

$\sigma_0$	Bulk tension
$\sigma_y$	Yield stress
$a$	Contact half width
$d$	Slip zone size
$d_0$	Internal length scale of the asymptotic stress fields
$f$	Coefficient of friction
$K_{II}$	Mode II stress intensity factor
$L_I$	Asymptotic multiplier for square root bounded pressure field
$L_{II}$	Asymptotic multiplier for square root bounded shear field
$P$	Normal force applied to contact
$Q$	Shear force applied to contact
$r, \theta$	Polar coordinates
$r_p$	Plastic radius
$s$	Distance along the line of contact, measured from the edge
$x, y$	Cartesian coordinates

## **1. Introduction**

Fretting fatigue is a material damage phenomenon that occurs when two bodies in contact are subjected to reciprocating shear loading. The prediction of fretting fatigue life is of great importance to a number of industries, and as such creating a model of fretting fatigue damage that encapsulates the major contributing factors has been a subject of much academic interest for a number of years. Some, such as the theory of critical distances [Zabala et al, 2020] focus on finding the state of stress in a region surrounding the edge of the fretting contact, but one model that has been the subject of much interest for many years is the “crack analogue” concept, as discussed in [Chambon and Journet, 2006], which uses concepts from linear elastic fracture mechanics to treat the growth of cracks from the edge of a contact as a crack turning or crack branching phenomenon.

In a very prescient paper published more than twenty years ago, Giannakopoulos, [1998] argued that there was a strong equivalence between the state of stress adjacent to a contact edge and that present at a crack tip. The paper was very thought-provoking, but it was not immediately apparent whether the authors intended these ideas to be used where the contact under consideration was in the form of a flat-faced rigid punch, or whether they were to be applied to incomplete contacts. In fact, the rigid punch comparison produces only a true match of asymptotic stress fields with a crack tip if the counterbody is incompressible, whereas if the contacting bodies are made from the same material but are convex so that the resulting contact is incomplete, perhaps surprisingly the analogy may potentially be stronger. We say ‘surprising’ because, at the edges of incomplete contacts, the contact pressure must fall smoothly to zero, and hence the attendant shear traction is limited by friction and so it, too, must also fall to zero. Therefore one might expect the comparison with the singular field at a sharp crack tip to be poor, but this is not necessarily so.

Imagine, first, that the coefficient of friction between the bodies is extremely high, sufficient to prevent all slip, Figure 2, so that when a shear force is applied the local state of stress is necessarily square root singular. If each body is capable of being idealised as a half-plane, the spatial distribution of stress is exactly the same as a mode II crack field. The stress concentration adjacent to contact edges may be relieved by either frictional slip or plastic slip. When it is the latter then there will be a whole area (in two dimensions) of plasticity which will straddle the contact interface.

We might wish to analyse the possibilities of frictional and plastic slip separately, and to start off in an approximate way, simply by considering violations of the frictional law (assuming the pair of bodies to be stuck everywhere) and the yield condition (assuming the material to be infinitely elastic). We do not expect there to be gross plasticity, but cyclic plasticity on a small scale with attendant irreversibilities which give rise to material degradation and the nucleation of cracks. If we have a weak material and strong friction we might expect the frictional slip zone to be buried well within the plastic zone, and therefore for the contact edge to behave as a monolithic notch. If the problem is one of a half-plane (convex) contact the notch becomes a crack, albeit one where the normal dominant eigensolution is square root bounded but, more importantly, the reversing mode II solution is symmetrical and, as stated earlier, the same as that at a crack tip. Nucleation of cracks from this region - small scale slip - becomes one of crack branching - the branch being a conventional opening mode I. On the other hand if the material is strong and the coefficient of friction weak the slip zone will be bigger than the implied plastic zone and, indeed, the process zone may be significantly smeared out or modified by slip. This, then, would truly be a fretting generated crack whereas the small-slip problem becomes one of branching of an existing crack.

This paper provides an objective comparison between the plastic slip zone shape and size at a contact edge and that at a crack tip, and looks at the former with and without frictional slip.

## 2. Implied Plastic Zone size and Shape

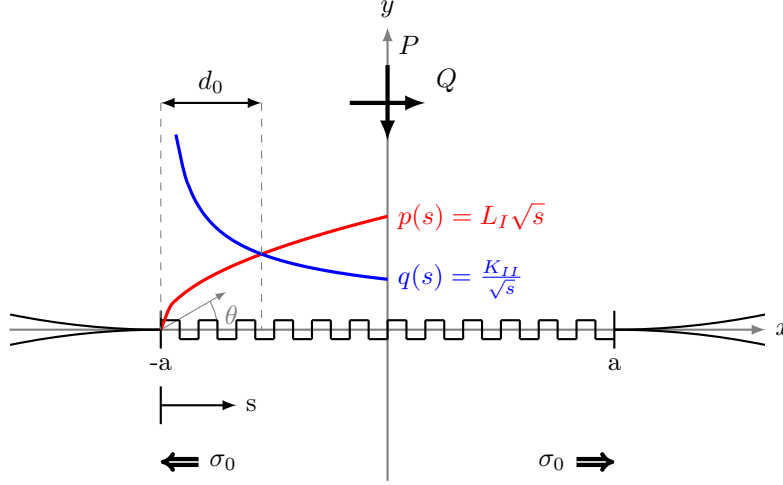


Figure 2: A diagram of the geometry for the fully stuck case showing loads and local stress asymptotes

If we have an incomplete contact between two elastically similar bodies of half width  $a$ , the shear stress,  $q(x)$ , along the contact interface induced by a shear force,  $Q$ , and a tension in one body of magnitude  $\sigma_0$  is given by

$$q(x) = \frac{Q}{\pi\sqrt{a^2 - x^2}} \pm \frac{\sigma_0 x}{4\sqrt{a^2 - x^2}} \quad (1)$$

when all slip is prohibited. We may write down the local state of stress at the contact edge in the form

$$q(s) = \frac{K_{II}}{\sqrt{s}}, \quad (2)$$

where  $s$  is a coordinate measured inwards from the contact edge and

$$K_{II} = \frac{Q}{\pi\sqrt{2a}} + \frac{\sigma_0}{4} \sqrt{\frac{a}{2}}. \quad (3)$$

Similarly, the normal load induces a contact pressure,  $p(s)$ , which falls smoothly to zero at the contact edge in a square root bounded manner, i.e.

$$p(s) = L_I \sqrt{s} \quad (4)$$

where  $L_I$  is a geometry-dependent multiplier and is given by, for example

$$L_I = \frac{P}{\pi} \sqrt{\frac{8}{a^3}} \quad (5)$$

where  $P$  is the normal load, for a Hertzian contact [Hills, et al 2016].

The mode II crack tip stress field is given by (note that these equations differ by a factor of  $\sqrt{2\pi}$  from the standard crack tip solutions because we don't include that factor in our definitions of the stress intensity factor)

$$\begin{pmatrix} \sigma_{rr} \\ \sigma_{\theta\theta} \\ \sigma_{r\theta} \end{pmatrix} = \frac{K_{II}}{\sqrt{r}} \begin{pmatrix} -\frac{5}{4}\sin\frac{\theta}{2} + \frac{3}{4}\sin\frac{3\theta}{2} \\ -\frac{3}{4}\sin\frac{\theta}{2} - \frac{3}{4}\sin\frac{3\theta}{2} \\ \frac{1}{4}\cos\frac{\theta}{2} + \frac{3}{4}\cos\frac{3\theta}{2} \end{pmatrix} \quad (6)$$

and the stress field from a  $L_I$  bounded asymptote is given by [Nils Cwiekala, Private conversation]

$$\begin{pmatrix} \sigma_{rr} \\ \sigma_{\theta\theta} \\ \sigma_{r\theta} \end{pmatrix} = L_I \sqrt{r} \begin{pmatrix} -\frac{3}{4}\cos\frac{\theta}{2} - \frac{1}{4}\cos\frac{5\theta}{2} \\ -\frac{5}{4}\cos\frac{\theta}{2} + \frac{1}{4}\cos\frac{5\theta}{2} \\ -\frac{1}{4}\sin\frac{\theta}{2} + \frac{1}{4}\sin\frac{5\theta}{2} \end{pmatrix} \quad (7)$$

where in plane strain

$$\sigma_{zz} = \nu(\sigma_{rr} + \sigma_{\theta\theta}) \quad (8)$$

so that Von Mises' criterion is

$$2\sigma_y^2 = (\sigma_{rr} - \sigma_{\theta\theta})^2 + (\sigma_{\theta\theta} - \sigma_{zz})^2 + (\sigma_{zz} - \sigma_{rr})^2 + 6\sigma_{r\theta}^2. \quad (9)$$

Considering the effect of just the  $K_{II}$  loading we can write that along the line  $\theta = 0$ , which is both the possible line of frictional slip and the line along which the plastic front,  $r_p(\theta)$ , extends furthest,

$$\frac{2r_p(0)\sigma_y^2}{K_{II}^2} = 6 \quad (10)$$

independent of the transverse constraint, because a state of pure shear exists. Under oscillatory loading of magnitude  $\Delta K_{II}$  shakedown will reduce the implied size of the shear stress by a factor of 4 (or we might think of this as replacing  $\sigma_y$  by  $2\sigma_y$  to give the range of stress which might be accommodated), to give, in the steady state

$$r_p(0) = \frac{3}{4} \left( \frac{\Delta K_{II}}{\sigma_y} \right)^2, \quad (11)$$

which is indicative of the size of the plastic slip zone, but we also wish to examine its shape. If we have just mode II loading of either the contact edge or the crack tip it is straightforward to include information about the size of the implied plastic zone, which is self similar, and this is addressed in many undergraduate textbooks. Re-write equation (6) in the contracted form

$$\sigma_{ij}(r, \theta) = \frac{K_{II}}{\sqrt{r}} f_{ij}^{II}(\theta) \quad (12)$$

and so

$$2r_p(\theta) \left( \frac{\sigma_y}{K_{II}} \right)^2 = (f_{rr}^{II}(\theta) - f_{\theta\theta}^{II}(\theta))^2 + (f_{\theta\theta}^{II}(\theta) - f_{zz}^{II}(\theta))^2 + (f_{zz}^{II}(\theta) - f_{rr}^{II}(\theta))^2 + 6f_{r\theta}^{II2}, \quad (13)$$

from which we may easily plot the shape of the normalised plastic zone. But the problem is more subtle if we have, also, a bounded pressure field present and so, in lieu of (12), the state of stress is given by

$$\sigma_{ij}(r, \theta) = \frac{K_{II}}{\sqrt{r}} f_{ij}^{II}(\theta) + L_I \sqrt{r} g_{ij}^I(\theta), \quad (14)$$

but we know that  $K_{II}[FL^{-3/2}]$  and  $L_I[FL^{-5/2}]$  so can bring out the internal length dimension, say  $d_0$ , by writing

$$d_0 = \left( \frac{K_{II}}{L_I} \right) \quad (15)$$

and so if we take equation (14) and divide through by  $\sqrt{K_{II}L_I}[FL^{-2}]$  we see it may be re-written in the form

$$\frac{\sigma_{ij}(r, \theta)}{\sqrt{K_{II}L_I}} = \sqrt{\frac{d_0}{r}} f_{ij}^{II}(\theta) + \sqrt{\frac{r}{d_0}} g_{ij}^I(\theta). \quad (16)$$

This is an extremely convenient form for the solution because it separates out the effect of the magnitude of the load ( $\sqrt{K_{II}L_I}$ ) and the internal length scale,  $d_0$ . The expression for the plastic radius is now very much more complicated, but is capable of being written down in terms of a single parameter. Let

$$h_{ij} \left( \theta; \frac{r}{d_0} \right) = \sqrt{\frac{d_0}{r}} f_{ii}^{II}(\theta) + \sqrt{\frac{r}{d_0}} g_{ii}^I(\theta) - \sqrt{\frac{d_0}{r}} f_{jj}^{II}(\theta) - \sqrt{\frac{r}{d_0}} g_{jj}^I(\theta) \quad (17)$$

so that the plastic radius  $r_p(\theta)/d_0$  is given by

$$2 \frac{\sigma_y^2}{K_{II}L_I} = h_{r\theta}^2 \left( \theta; \frac{r_p}{d_0} \right) + h_{\theta z}^2 \left( \theta; \frac{r_p}{d_0} \right) + h_{zr}^2 \left( \theta; \frac{r_p}{d_0} \right) + 6 \left[ \sqrt{\frac{d_0}{r_p}} f_{r\theta}^{II}(\theta) + \sqrt{\frac{r_p}{d_0}} g_{r\theta}^I(\theta) \right]^2. \quad (18)$$

### 3. Results - No slip comparison of implied plastic fields

The question arises ‘What is a realistic choice of  $d_0$ ?’ and one way of answering this might be to attach the solution to a specific finite geometry, for example Hertz’ problem. Substituting the calibrations for  $L_I, K_{II}$  into (15) we see that

$$\frac{d_0}{a} = \frac{Q}{4P} \quad (19)$$

Therefore, when there is no applied shear force  $d_0 \rightarrow 0$  (so that the effect of the shear load vanishes, and the normal load dominates the problem). If we assume typical coefficients of friction for alloys we might expect the maximum value of  $Q/P$  to be around 1/2 if the contact is in partial slip so that the maximum value of  $d_0/a$  is about 1/8. Looking at the magnitude of the load we see that this is characterised by the left hand side of equation (18) and, making use of (3,5)

$$\frac{K_{II}L_I}{\sigma_y^2} = \frac{8}{\pi^2} \left( \frac{Q}{2a\sigma_y} \right) \left( \frac{P}{2a\sigma_y} \right) \quad (20)$$

In a real contact we might expect the maximum nominal contact pressure to be just about equal to the yield stress so that the right hand side of this equation, for maximum nominal shear force as above will be about  $4/\pi^2$  or just under 0.5.

Contours of the position of the implied plastic front for various values of  $\frac{K_{II}L_I}{\sigma_y^2}$  are plotted over normalised  $\left( \frac{x}{d_0}, \frac{y}{d_0} \right)$  space in Figure 3 under conditions of plane strain with  $\nu = 0.3$ . The definition of  $x$  and  $y$  in this figure differ from those used in figure 2, the coordinate system is attached to the edge of the contact, rather than it's centre. It should be noted that there are two plastic zones present, a distorted version of the distinctive 'figure of eight' plastic zone associated with a  $K_{II}$  stress field growing outwards from  $r = 0$  and a 'c' shaped plastic zone associated with an  $L_I$  stress field growing inwards from  $r = \infty$ , with the boundary  $r = d_0$  providing a rough partition between these two zones.

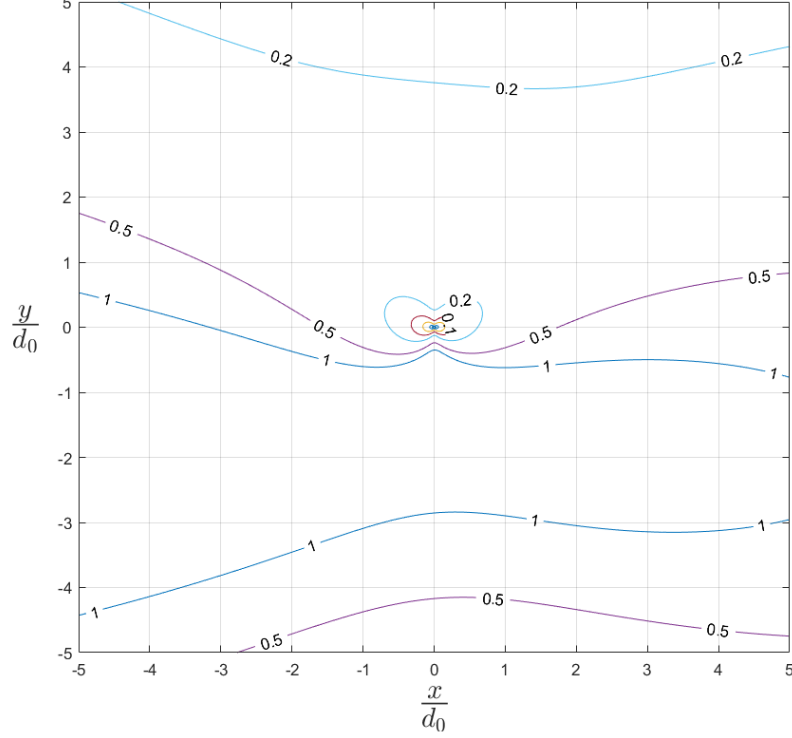


Figure 3: Contours of the implied plastic front for various values of normalised applied load  $\frac{K_{II}L_I}{\sigma_y^2}$ .

Figure 4 provides a plot of the implied plastic zone front shape in the region  $r < d_0$ , and the nearest ‘pure mode  $II$ ’ ie. crack tip field for comparison. The latter is found in the following way: we ‘open out’ the polar plot and display, in Cartesian form,  $r_p(\theta)$  for  $-\pi < \theta < \pi$  for the contact edge. We then think of a second representation, viz. the crack tip  $K_{II}$  field, but where the magnitude of the best choice of the multiplier is initially left as a parameter whose magnitude (i.e. the multiplier  $\frac{K_{II}L_I}{\sigma_y^2}$ ) is found by doing a least-squares fit, and where the correlation coefficient provides a rigorous measure of the proximity of the contact edge field to the crack tip field. For each pair of these contours the coefficient of determination,  $R^2$ , was calculated to ascertain the quality of the fit. These are given in table 1. The  $K_{II}$  stress field is normalised in exactly the same way as the combined  $L_I + K_{II}$  stress field, and values of  $\frac{K_{II}L_I}{\sigma_y^2}$  are provided for comparison.

$R^2$  is defined as



$$R^2 = 1 - \frac{SSR}{TSS} \quad (21)$$

where the sum of squares of the residuals is defined as

$$SSR = \sum [r(\theta_i) - f(\theta_i)]^2 \quad (22)$$

and the total sum of squares is defined as

$$TSS = \sum [r(\theta_i) - \bar{r}]^2 \quad (23)$$

in which  $r(\theta)$  is the plastic radius from the  $L_I + K_{II}$  stress field,  $\bar{r}$  is the average plastic radius from the  $L_I + K_{II}$  stress field and  $f(\theta)$  is the plastic radius from the best fitted pure  $K_{II}$  stress field. An  $R^2$  value of 1 implies a perfect fit between the  $L_I + K_{II}$  plastic zone and the pure  $K_{II}$  plastic zone, an  $R^2$  value of zero implies that the fitted  $K_{II}$  stress field has the same amount of variance as simply averaging the  $L_I + K_{II}$  plastic zone (i.e. fitting a circle) and negative values of  $R^2$  indicate that the fitted  $K_{II}$  plastic zone has higher variance than simply averaging the plastic radius.

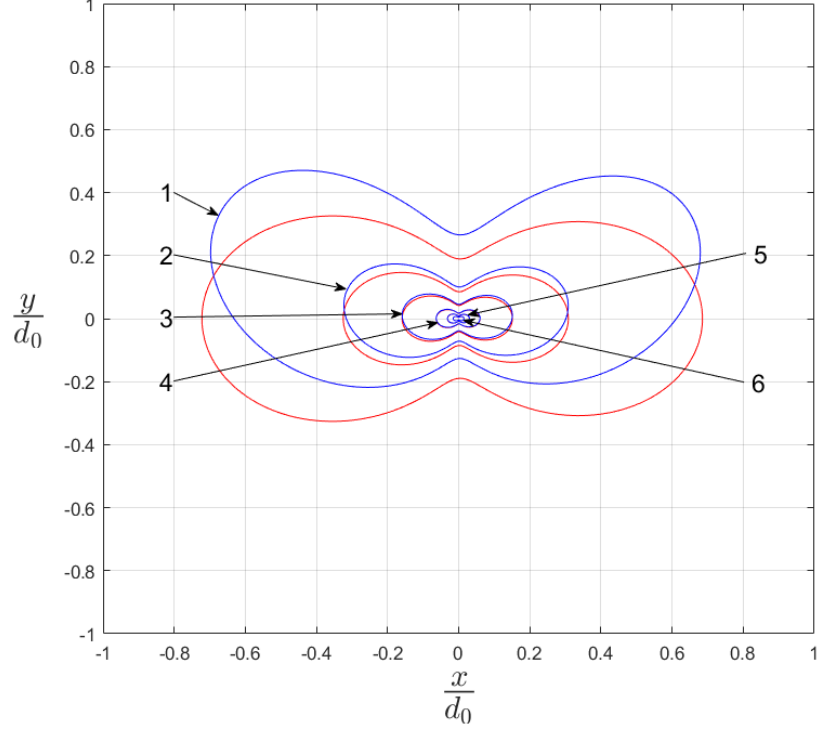


Figure 4: Comparison between combined  $L_I + K_{II}$  implied plastic fronts (Blue) and pure  $K_{II}$  implied plastic fronts (Red) for various values of  $\frac{K_{II}L_I}{\sigma_y^2}$ .

Contour	$\frac{K_{II}L_I}{\sigma_y^2}$ for $K_{II} + L_I$	$R^2$	$\frac{K_{II}L_I}{\sigma_y^2}$ for $K_{II}$
1	0.2	0.379	0.22847
2	0.1	0.864	0.10274
3	0.05	0.967	0.05033
4	0.02	0.995	0.02001
5	0.01	0.999	0.00999
6	0.005	0.999	0.00498

Table 1: A Table giving the coefficient of determination for each of the contours in 4.

#### 4. Small Scale Slip

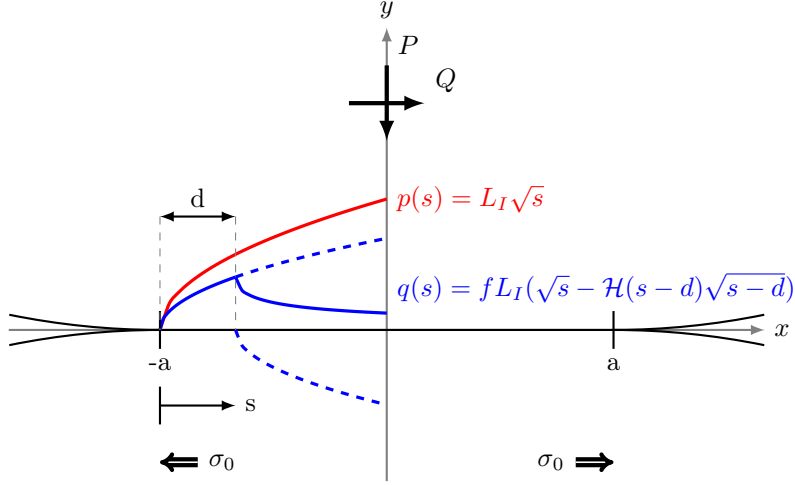


Figure 5: A diagram of the geometry for the partial slip case showing loads and local stress asymptotes

The steady state slip zone size,  $d$ , allowing, for frictional shakedown, is given by [Dini et al, 2005]

$$fd = \frac{\Delta K_{II}}{L_I} = d_0 \quad (24)$$

where  $f$  is the coefficient of friction, and the relative plastic and frictional slip extent is given by

$$\frac{r_p(0)}{d} = \frac{3f\Delta K_{II}L_I}{4\sigma_y^2}. \quad (25)$$

If  $r_p(0)/d > 1$  the plastic zone envelops the slipping region of the interface, and when this is true the frictional slip may have only a mild effect on crack nucleation. Under these conditions a fretting contact edge will behave like a notch of angle  $2\pi$ , i.e. a crack tip, as suggested by Giannakopoulos [Giannakopoulos et al, 2000]. We have just a constant normal pressure problem given by equation (4) together, in the limit, when  $f \rightarrow \infty$ , with a reversing singular field, where

$$\Delta q(s) = \frac{\Delta K_{II}}{\sqrt{s}} \quad (26)$$

This is as described above (in§1), except for the bounded pressure problem, which is constant in time and will, therefore, shake down. The solution provides an estimate of the plastic front position for a perfectly sticky interface, although there is a violation of the slip law over the region  $0 < s < d$ .

The other possibility is that slip envelops the plastic region. When  $\sigma_Y \rightarrow \infty$  the plastic zone will vanish. The normal contact solution is still given by (4), and the shear traction distribution in lieu of (2) will instead be given by [Dini et al, 2005]

$$q(s) = L_{II}\sqrt{s} - L_{II}\sqrt{s-d} = fL_I\sqrt{s} - fL_I\sqrt{s-d}. \quad (27)$$

as illustrated in figure 5, where  $\mathcal{H}(s-d)$  is the heaviside step function. The stress field from a square root bounded shear asymptote is given by [Nils Cwiekala, Private conversation]

$$\begin{pmatrix} \sigma_{rr} \\ \sigma_{\theta\theta} \\ \sigma_{r\theta} \end{pmatrix} = L_{II}\sqrt{r} \begin{pmatrix} \frac{3}{4}\sin\frac{\theta}{2} + \frac{5}{4}\sin\frac{5\theta}{2} \\ \frac{5}{4}\sin\frac{\theta}{2} - \frac{3}{4}\sin\frac{5\theta}{2} \\ -\frac{1}{4}\cos\frac{\theta}{2} + \frac{5}{4}\cos\frac{5\theta}{2} \end{pmatrix} \quad (28)$$

## 5. Plasticity Zone Calculation with Finite Slip

The ideas put forward in the last section may be investigated in more detail by looking at the implied size of the plastic front, again based on an elasticity solution plus violations of the yield criterion, but now for the elastic state of stress given by a slipping contact. This is readily achieved by superposing two bounded, sliding shear traction distributions separated by the slip zone length (equation (28)). We will again work in the framework of the normalisation devised for the full-stuck solution: the size of the steady state slip zone,  $d$ , is given by equation (24) and the internal length dimension,  $d_o$ , is given by equation (15).

The stress field is now given by

$$\sigma_{ij}(r, \theta) = L_{II} [\sqrt{r}g_{ij}^{II}(\theta) - \sqrt{\rho}g_{kl}^{II}(\phi)] + L_I\sqrt{r}g_{ij}^I(\theta) \quad (29)$$

where  $L_{II} = fL_I$ , ie.

$$\sigma_{ij}(r, \theta) = L_I [\sqrt{r}(g_{ij}^I(\theta) + fg_{ij}^{II}(\theta)) - f\sqrt{\rho}g_{kl}^{II}(\phi)] \quad (30)$$

and

$$\rho^2 = d^2 + r^2 - 2rd\cos\theta \quad \sin\phi = \sin\theta \left( \frac{r}{\rho} \right).$$

The stress components referenced by  $g_{kl}^{II}(\phi)$  have been rotated by  $\theta - \phi$  using the transformation law for the Cauchy stress tensor to ensure all stresses are in the same coordinate system.

Note that, although this appears superficially to be a square root bounded distribution the difference between two bounded terms separated by a (small) distance  $d$ , or  $d_o/f$  appears like a square root singular field when  $r \gg d$ .

Unlike the no slip case we cannot reduce the problem to a single parameter space; instead the plastic zone depends on two dimensionless parameters/groups,  $\frac{K_{II}L_I}{\sigma_y^2}$  and the coefficient of friction,  $f$ . Figure 6 shows contours of

$\frac{K_{II}L_I}{\sigma_y^2}$  for a coefficient of friction of 0.7. It can clearly be seen that in this case there is no evidence of the ‘figure of eight’ plastic zone normally associated with a  $K_{II}$  singular stress field.

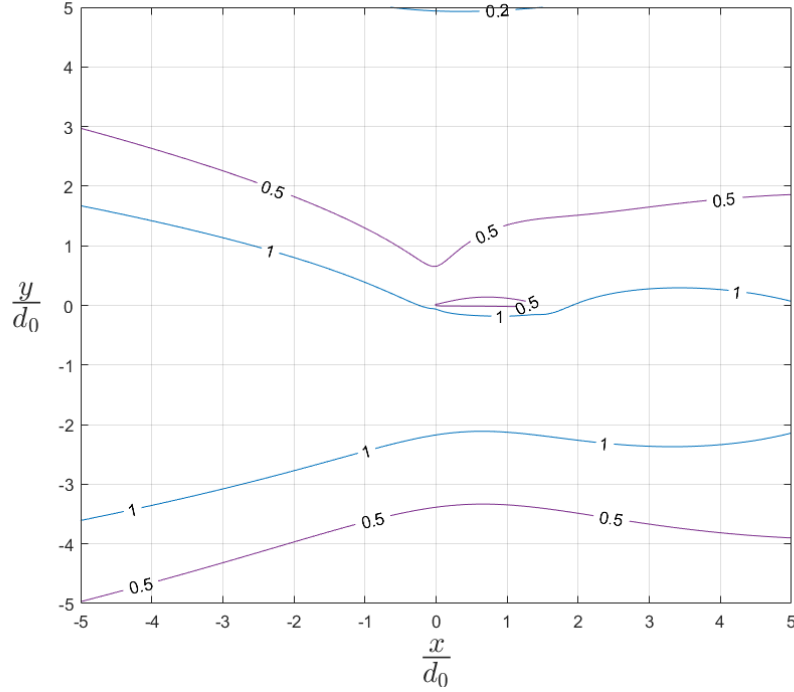


Figure 6: Implied plastic zones for values of  $\frac{K_{II}L_I}{\sigma_y^2}$  for the partial slip problem with  $f = 0.7$  ( $\frac{d}{d_0} \approx 1.4$ ).

## 6. Conclusion

In conventional fracture mechanics we require the extent of the plasticity zone to be small, sufficiently small for it to be surrounded wholly by a region in which the singular field controls the hinterland before higher order terms in a series expansion of the crack tip field start to become important. Equally, in the crack nucleation problem we generally require, at the contact edge, the plasticity zone to be sufficiently small for the hinterland to be controlled by the dominant singular term if that does, indeed control crack nucleation. In the case of a complete contact this means that we would require the plastic zone to be small enough to be controlled by the mode I eigensolution, but at an incomplete contact edge the problem is rather different. There is a constant bounded symmetric field (pressure) together with a singular anti-symmetric

oscillatory field. For the problem to behave like a crack tip the process zone must be smaller than the region where distortion to the nominal traction from  $K_{II}$  to  $L_I$  domination takes hold, and a good estimate of the boundary of the undistorted region is provided by  $d_0$ . Notice that the requirement is stronger than that from LEFM, as we require both the extent of the plasticity zone and the extent of frictional slip to be small.

So, provided that both requirements of small scale slip are satisfied we anticipate that the value of  $\Delta K_{II}$  will have a dominant effect on the nucleation process. The mode I field is also square root singular at a crack tip but is only square root bounded at an incomplete contact edge. We have a simple means, in this formulation, of quantifying what we mean by small scale slip; it is when the hinterland is controlled by the singular shear traction field, i.e. when  $r < d_0$ . Interpreted in terms of frictional slip, this means that  $d/d_0 < 1$ , or, from equation (29), that  $f > 1$  and this, is, of course, an impractical requirement. On the question of small scale plastic yield the maximum practical load may be more acceptable. If we use equation (11) and limit the maximum plastic radius to  $d_0$  this would mean that the requirement would be

$$\frac{r_p}{d_0} = \frac{3}{4} \frac{\Delta K_{II} L_I}{\sigma_y^2} < 1,$$

or

$$\frac{\Delta K_{II} L_I}{\sigma_y^2} < \frac{4}{3} \quad (31)$$

If we specialise to Hertz geometry and take representative values (equation 20) we know that a heavily loaded contact might give rise to a left hand side of this equation of about unity. So, frictional slip is a more concerning problem in terms of the fidelity of the mode II loading field.

In Figure 7 we show the dimensionless slip zone size and dimensionless plastic zone size for a range of practical experiments conducted on a range of geometries and with a wide range of materials [Dini, 2005b], [Szłowski, 1998], [Hojjati-Talemi et al, 2014], [Nowell, 1988]. The graph is partitioned into two regions, with the upper triangular region corresponding to tests where plasticity is dominant and the lower triangular region corresponding to tests where slip is dominant. Additionally, if the data point is sufficiently near the origin ( $\frac{r_p}{d_0} < 1, \frac{d}{d_0} < 1$ ) small scale plasticity and small scale slip apply and the problem is  $K_{II}$  field dominated. It can be seen that for all the data sets, except those from the low alloy steel tests, the plastic zone size is small enough to be considered as ‘small scale plasticity’ ( $\frac{R_p}{d_0} < 1$ ). In contrast none of the data sets have slip zones small enough for them to be considered as ‘small scale frictional slip’ ( $\frac{d}{d_0} < 1$ ) which reflects that very few real material combinations have coefficients of friction greater than 1. Due to these large slip zones none of the tests were performed in the region where the stress fields are  $K_{II}$  dominated (indicated by the square in the lower left corner of the chart) and the influence of the normal load is therefore likely to be important.

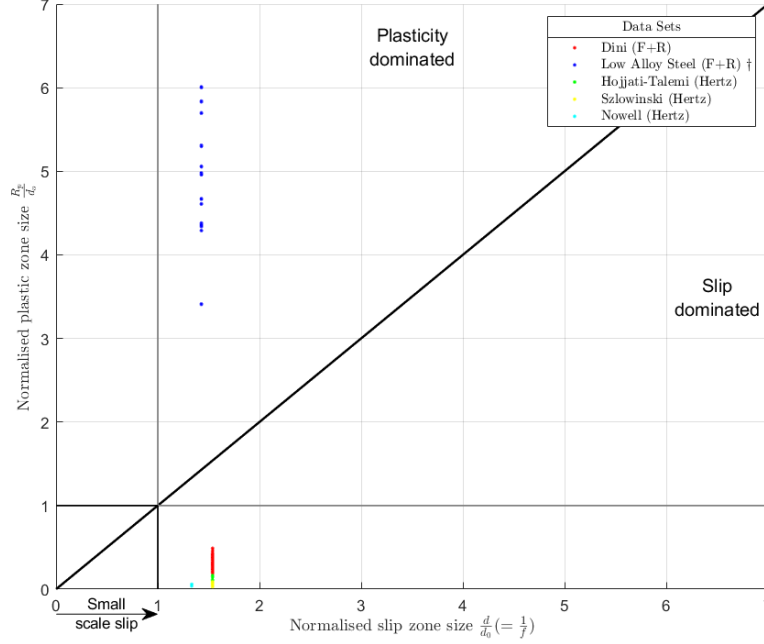


Figure 7: Various data sets plotted on axis of normalised plastic zone size and Normalised Slip zone size, and indicating the region over which the  $K_{II}$  Stress field dominates ( $r < d_0$ ).

## 7. References

- Zabala A, Infante-García D, Giner E, Goel S, Endrino J L, Llavori I (2020), On the use of the theory of critical distances with mesh control for fretting fatigue lifetime assessment, *Tribology International*, **142**, 105985
- Chambon L, Journet B (2006), Modelling of fretting fatigue in a fracture-mechanics framework, *Tribology International*, **39**, (10), 1220-1226
- Dini D, Sackfield A, Hills DA, (2005), Comprehensive bounded asymptotic solutions for incomplete contacts in partial slip, *Journal of Mechanics and Physics of Solids*, **53**, 437-454, ISSN: 0022-5096
- Giannakopoulos A E, Lindley TC, Suresh S,(1998) Aspects of equivalence between contact mechanics and fracture mechanics: theoretical connections and a life prediction methodology for fretting Fatigue. *Acta Mater.*, **46**, (9) 2955-2968.
- Giannakopoulos A E, Venkatesh T C, Suresh S, Chenut C, (2000) Similarities of stress concentrations in contact at round punches and fatigue at notches: implications to fretting fatigue crack initiation, *Fatigue & Fracture of Engineering Materials & Structures*, **23**, 561-571

Hills D A, Fleury R M N, and Dini D, (2016), Partial slip incomplete contacts under constant normal load and subject to periodic loading *International Journal of Mechanical Sciences*, **108–109**,115-121.

Dini D and Dyson I, (2005b), Fretting Fatigue test results for Ti 6/4 (D4.1), Analysis of results and validation of assessment criteria (D5.2): issue 2, UTC Report No. 219, University of Oxford

Szolwinski M P, Farris T N, (1998), Observation, analysis and prediction of fretting fatigue in 2024-T351 aluminum alloy, *Wear*, **221**, 24–36

Hojjati-Talemi R, Wahab M A, De Pauw J, De Baets P, (2014), Prediction of fretting fatigue crack initiation and propagation lifetime for cylindrical contact configuration, *Tribology International*, **76**, 73-91

Nowell D, (1988), An analysis of Fretting Fatigue, DPhil Thesis, University of Oxford

## 8. Acknowledgements

James Truelove expresses with thanks the award of an iCASE award ref 17000027 from Rolls-Royce plc which has enabled him to carry out this work.

We would also like to thank TechnipFMC for allowing us to use data collected as part of a project at the University of Oxford in the creation of figure 7 (†)